

Article

A pseudo five-fold symmetrical ligand drives geometric frustration in porous metal-organic and hydrogen bonded frameworks

Frederik Haase, Gavin A. Craig, Mickaele Bonneau, Kuniyoshi Sugimoto, and Shuhei Furukawa

J. Am. Chem. Soc., **Just Accepted Manuscript** • DOI: 10.1021/jacs.0c04450 • Publication Date (Web): 15 Jul 2020

Downloaded from pubs.acs.org on July 16, 2020

Just Accepted

“Just Accepted” manuscripts have been peer-reviewed and accepted for publication. They are posted online prior to technical editing, formatting for publication and author proofing. The American Chemical Society provides “Just Accepted” as a service to the research community to expedite the dissemination of scientific material as soon as possible after acceptance. “Just Accepted” manuscripts appear in full in PDF format accompanied by an HTML abstract. “Just Accepted” manuscripts have been fully peer reviewed, but should not be considered the official version of record. They are citable by the Digital Object Identifier (DOI®). “Just Accepted” is an optional service offered to authors. Therefore, the “Just Accepted” Web site may not include all articles that will be published in the journal. After a manuscript is technically edited and formatted, it will be removed from the “Just Accepted” Web site and published as an ASAP article. Note that technical editing may introduce minor changes to the manuscript text and/or graphics which could affect content, and all legal disclaimers and ethical guidelines that apply to the journal pertain. ACS cannot be held responsible for errors or consequences arising from the use of information contained in these “Just Accepted” manuscripts.

A pseudo five-fold symmetrical ligand drives geometric frustration in porous metal-organic and hydrogen bonded frameworks

Frederik Haase,^{*,a} Gavin A. Craig,^a Mickaële Bonneau,^a Kunihisa Sugimoto,^{a,b} Shuhei Furukawa^{*,a,c}

^a Institute for Integrated Cell-Material Sciences (WPI-iCeMS), Kyoto University, iCeMS Research Bldg, Yoshida, Sakyo-ku, Kyoto 606-8501, Japan

^b Japan Synchrotron Radiation Research Institute/SPRING-8, Kouto, Sayo, Hyogo 679-5198, Japan

^c Department of Synthetic Chemistry and Biological Chemistry, Graduate School of Engineering, Kyoto University, Katsura, Nishikyo-ku, Kyoto 615-8510, Japan

ABSTRACT: Reticular framework materials thrive on designability, but unexpected reaction outcomes are crucial in exploring new structures and functionalities. By combining “incompatible” building blocks, we employed geometric frustration in reticular materials leading to emergent structural features. The combination of a pseudo C_5 symmetrical organic building unit based on a pyrrole core, with a C_4 symmetrical copper paddlewheel synthon led to three distinct frameworks by tuning the synthetic conditions. The frameworks show structural features typical for geometric frustration: self-limiting assembly, internally stressed equilibrium structures and topological defects in the equilibrium structure, which manifested in the formation of a hydrogen bonded framework, distorted and broken secondary building units and dangling functional groups, respectively. The influence of geometric frustration on the CO_2 sorption behavior and the discovery of a new secondary building unit shows geometric frustration can serve as a strategy to obtain highly complex porous frameworks.

INTRODUCTION

Reticular framework materials are a class of materials that are constructed by the selection or design of building blocks and linkage groups such that a desired net is formed.¹ This approach is successfully applied for the introduction of functionality on the organic linkers and on known metal based secondary building units (SBU),² while structural complexity can be increased by the rational construction of new organic nodes and new nets³ or by the synthesis of controlled multivariate materials.^{4–6} Recently, design strategies have emerged that seek to deviate from this approach and attempt to increase complexity by introducing well-defined defects and mismatches into the backbone that lead to reduced symmetry, new nets and open metal sites.¹ This can be achieved by linker clip-off,⁷ dissolution and introduction of defects^{8–11} or the installation of size and shape mismatched linkers.¹ These approaches are all based on the knowledge of a well-defined parent lattice. Our strategy here is to use mismatched symmetry in order to introduce geometric frustration, where the mismatch is large enough to prohibit the formation of predetermined lattices or nets. Geometric frustration arises when local geometric constraints hinder the energetic minimization of all of the interactions at the same time.¹² This is a sought after phenomenon for spin ices in magnetic materials¹³ and their application in data storage,¹⁴ but the

use of competing interactions to obtain complex systems is a widespread phenomenon.¹³ We therefore wanted to induce geometric frustration, in order to explore new emergent structures and features^{13,15} without preconception of the reaction outcome.

In this work, we introduced geometric frustration through a linker with pseudo- C_5 symmetry, as the symmetry cannot be propagated to a classical periodic lattice based on translation, while periodic lattices based on rotation and translation such as in a quasicrystal could support this symmetry.^{12,16} Several strategies exist for the introduction of C_5 symmetry in organic building blocks,^{17–20} as these are used for the synthesis of large cage coordination compounds,^{19,21–24} or as metal nodes for the synthesis of quasicrystal approximants.²⁵ As introducing C_5 -symmetry can be synthetically challenging,^{20,26} instead we designed a pseudo- C_5 symmetrical ligand based on a pyrrole core (see method section, Figure S2). The pseudo- C_5 symmetric linker containing pendant carboxylic acid groups, 1,2,3,4,5-penta (4-(benzoic acid))pyrrole (**pLH₅**; Figure 1) was reacted with copper(II) ions with the intention of creating the C_4 -symmetric paddlewheel motif. While metal-organic frameworks based on paddlewheel have been reported with planar 2-c,²⁷ 3-c,²⁸ 4-c²⁹ and 6-c³⁰ nodes before, a search of MOF databases³¹ revealed no nets with alternating 5-c and 4-c nodes. The combination of

C_4 and C_5 local symmetries was, therefore, expected to be difficult to reconcile while maintaining the symmetry of the building blocks.

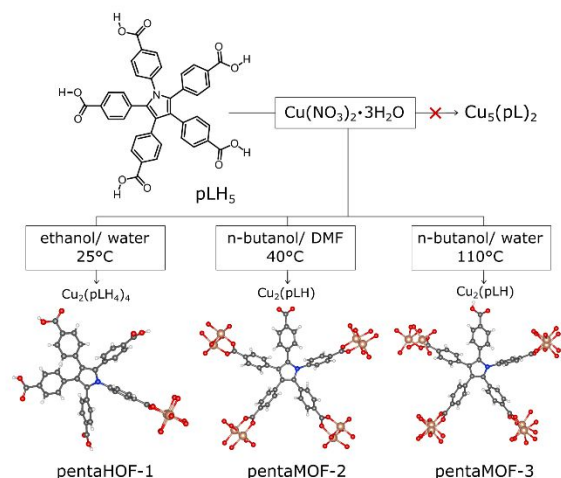


Figure 1. Schematic illustration of the synthesis of materials from the pentagonal linker pLH_5 .

RESULTS AND DISCUSSION

Structural description of three frameworks based on the pentagonal linker. Using pLH_5 for the synthesis of frameworks, three materials were crystallized: a hydrogen bonded framework (HOF), based on a molecular copper(II) complex containing four $[\text{pLH}_4]^-$ units ($\text{Cu}_2(\text{pLH}_4)_4$; pentaHOF-1) and two different metal-organic frameworks (MOF) consisting of $[\text{pLH}]^{4-}$ units ($\text{Cu}_2(\text{pLH})$; pentaMOF-2 and pentaMOF-3). The materials differ in their connectivity, node-distortion, porosity and linker-to-linker contacts, which point towards the pathways in which the frustration is released in this system.

The interdiffusion of an aqueous copper nitrate solution with a solution of pLH_5 in ethanol at room temperature leads to the formation of a metal containing HOF (pentaHOF-1). This material consists of a molecular copper complex $\text{Cu}_2(\text{pLH}_4)_4$ that is composed of a single copper paddlewheel surrounded by four $[\text{pLH}_4]^-$ moieties in a propeller shape (Figure 2a). The pentaHOF-1 crystallizes in the tetragonal space group $P4/nnc$ (Table S1) in which the $\text{Cu}_2(\text{pLH}_4)_4$ molecules arrange to form a square lattice layer. The layers are stacked in an alternating fashion to form a distorted body centered arrangement (Figure 2b). The structure is stabilized by hydrogen bonding interactions where one $\text{Cu}_2(\text{pLH}_4)_4$ molecule interacts with 10 of its neighbors (8 from the body centered arrangement and 2 from interaction with the molecules above and below the $\text{Cu}_2(\text{pLH}_4)_4$ molecules; Figure S3) through its 16 carboxylic acids. The structure contains a disordered hydrogen bonding motif where four carboxylic acids meet. The disorder can be disentangled to two binding modes (Figure S4), where either four carboxylic acids form three hydrogen bonds or two carboxylic acid pairs can form one hydrogen bond each. The oxygen-oxygen distances and the angles between the carboxylic acids are in line with moderately strong hydrogen bonds (Table

S2).³² The pentaHOF-1 structure contains two types of 1D channels parallel to the c -axis. The first type is purely intermolecular, created between stacks of $\text{Cu}_2(\text{pLH}_4)_4$ molecules with pore apertures of $11.3 \times 11.3 \text{ \AA}^2$ (indicated as A in Figure S5). The second type of void is created by connecting the inter-molecular voids within one stack of molecules by small intramolecular apertures ($4.6 \times 3.8 \text{ \AA}^2$) (indicated as B in Figure S5).

Changing the solvent system led to the formation of a MOF with the composition $\text{Cu}_2(\text{pLH})$. pentaMOF-2 single crystals were obtained with monoclinic crystal system in the $C2/c$ space group by reaction in a mixture of dimethyl formamide (DMF) and n -butanol heated at 40°C. The structure is composed of a fully 3D metal-organic network containing $[\text{pLH}]^{4-}$ units and copper paddlewheels. Two out of four carboxylate groups create a square lattice layer with regular copper paddlewheels (Figure 2c), while the remaining two carboxylate groups twist out of plane and connect these layers with a distorted copper paddlewheel leading to a **sqc176**³³ (lvt) topology (Figure 2d). The fifth, potential carboxylate group remains protonated and is therefore not involved in binding to copper. The carboxylic acid group protrudes into the interstitial voids and has an average $d_{\text{O} \cdots \text{O}}$ of 6.19 Å to the nearest free carboxylic acid. It is therefore not able to participate in hydrogen bonding to the MOF backbone. Individual linker molecules in the structure are not in contact with each other and are separated by solvent molecules, which could be resolved by SXR D (Figure S6). The close proximity of the linkers without close contact leads to a three-dimensional pore structure in pentaMOF-2 with small diameter accessible voids (Figure S7).

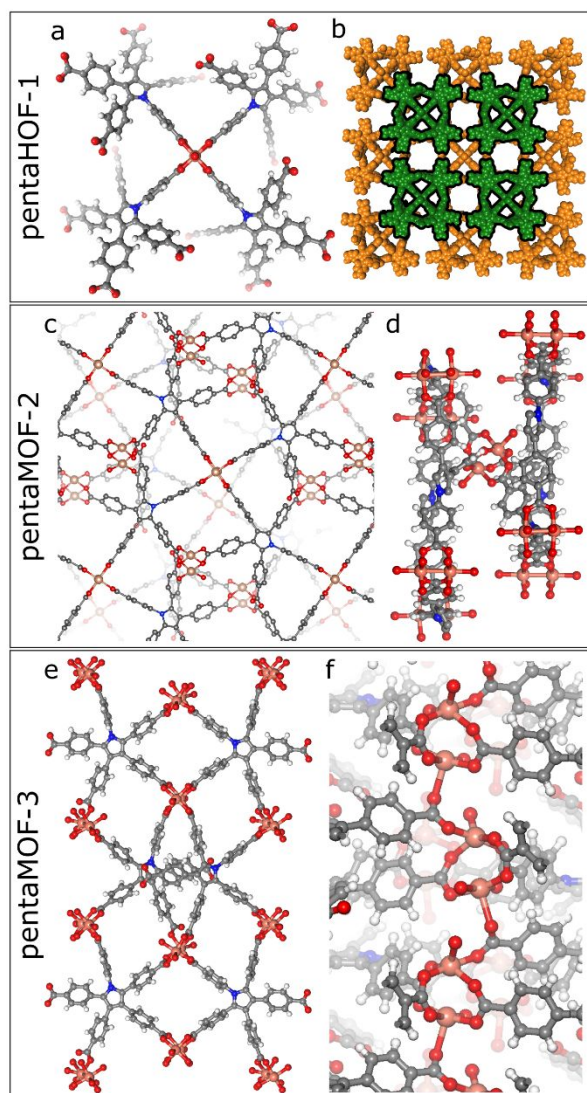


Figure 2. Detail illustrations of the crystal structures of (a,b) pentaHOF-1, (c,d) pentaMOF-2 and (e,f) pentaMOF-3, which emphasize the connectivity of the structure.

By increasing the reaction temperature up to 110°C and using an n-butanol/water mixture, we obtained single crystals of pentaMOF-3 in an orthorhombic $Pna2_1$ space group (Table S1) with the same composition $Cu_2(pLH)$ as pentaMOF-2, but with a different connectivity. The structure is composed of $[pLH]^{4-}$ units where four of the five available carboxylates bind to copper and lead to the formation of a two-dimensional layer with a distorted square lattice net (Figure 2e). The remaining fifth carboxylate is protonated and is able to form moderately strong hydrogen bond with a second linker.³² The carboxylic acid is disordered, with one state resembling a typical carboxylic acid dimer with two hydrogen bonds, and another state a carboxylic acid dimer where only one hydrogen bond can be formed (Table S2, Figure S8) The copper binds the linker with two distinct secondary building units (SBU). The first is a regular copper paddlewheel, albeit a distorted one. The second SBU contains pairs of copper ions that resemble a copper paddlewheel only in three of four carboxylates, while the fourth carboxylate group

coordinates to one copper in an equatorial fashion and through pseudo-coordination to the axial position of a neighboring copper pair, thus leading to a one-dimensional SBU (Figure 2f). The copper pairs are bridged by three axial carboxylate anions with a d_{Cu-Cu} 2.98 Å, which is considerably larger than in the regular paddlewheels present in the structure with $d_{Cu-Cu} = 2.64$ Å. The inter-pair distance, bridged by an axial-equatorial carboxylate binding motif is even larger with $d_{Cu-Cu} = 4.67$ Å. The pseudo-coordination of the rod SBU and the hydrogen bonding connect the individual layers with each other, leading to a 3D net based on the **sqc54**³³ topology (Figure S9). The structure contains small undulating 1D channels with an aperture of $5.5 \times 3.6 \text{ \AA}^2$ (Figure S10).

Nets. The net of the pentaHOF-1 can be described by simplifying the structure by different degrees. The copper paddlewheel is a 4-c node the pL presents a 5-c node and the hydrogen bonded node can be considered as a 4-c node on arrives at a 4,4,5-c net with a transitivity of (3 3) (Figure S11). However, since the bonding situation is ambiguous due to disorder, the hydrogen bonded node can also be considered as a linear connection, thus a 4,5-c net is obtained with a transitivity of (2 2) as two kinds of edges are observed in this structure. In this structure the nodes are not alternating, like in many other observed 4,5-c nets.³¹ When considering the hydrogen bonded node as a 4-c node, the question arises, why no additional paddlewheel is formed in this position, which would lead to the compound Cu_5pL_2 . When constructing a model of Cu_5pL_2 with the same 4,4,5-c net, the paddlewheel placed instead of the hydrogen bonded node is highly strained (Figure S12). This node is much more distorted than pentaMOF-2 and pentaMOF-3 paddlewheels. The highly distorted coordination environment might prohibit the formation of a copper paddlewheel. This might explain why the hydrogen bonded framework pentaHOF-1 is formed instead of Cu_5pL_2 . As the formation of an edge transitive 4,5-c net might not be possible,³⁷ the 4,4,5-c net is a plausible candidate for Cu_5pL_2 . The proposed structure is however only one possibility for the net and others are unknown. Attempts to obtain Cu_5pL_2 were unsuccessful, with increasing the reaction temperature or introducing base only leading to pentaMOF-3. The assembly of the hydrogen bonded molecules can also be considered as just molecules that connect to neighboring molecules. This leads to a 10-c unimodal net obtained with a transitivity (1 2) **bct**.

The change in connectivity from a 5-c node to a 4-c node as observed in the structures of penta-MOF-2 and pentaMOF-3 also have a profound effect on the nets of the materials. While the pentaMOF-2 crystallized with a **lvt** net which is based on only 4-c nodes, the pentaMOF-3 crystallizes with 2-periodic **sql** net layers, which are however connected through the rod SBU leading to a 6-c node instead of a 4-c node in one half of the available copper paddlewheels. This leads to a three-dimensional periodic **sqc54** net.

Sorption properties of framework materials. The single crystal structures of the materials presented here showed promising solvent accessible voids, and we

therefore investigated gas sorption properties. Only the pentaHOF-1 showed uptake of N_2 at 77 K with a type-I isotherm, with a BET surface area of $849 \text{ m}^2\text{g}^{-1}$ (Figure 3a), which confirms its permanent porosity.

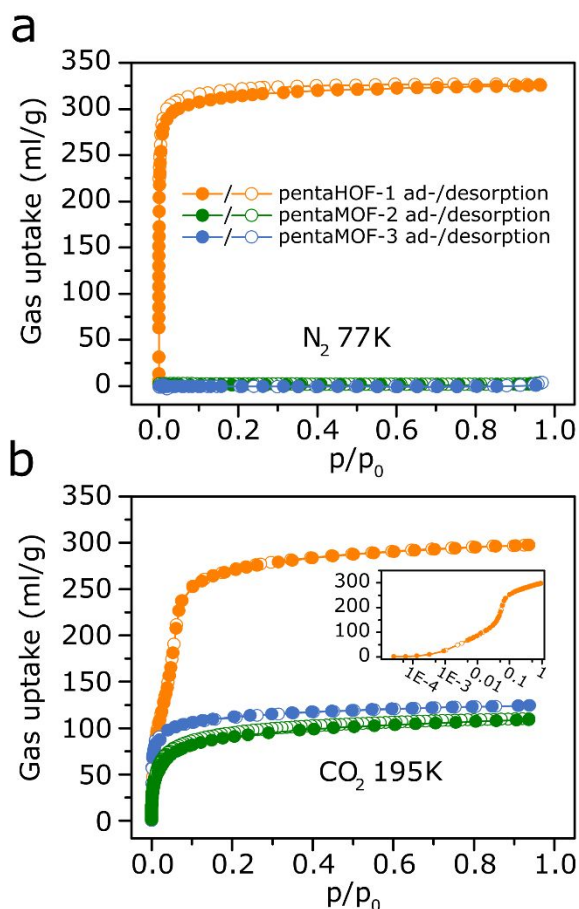


Figure 3. Sorption measurement of pentaHOF-1, pentaMOF-2 and pentaMOF-3 for (a) N_2 at 77 K and (b) CO_2 at 195 K.

In contrast, all three materials showed CO_2 adsorption at 195K. The isotherm of pentaHOF-1 exhibits a steep rise at low partial pressures that includes a step at around $0.055 P/P_0$ (Figure 3b, inset). Such a stepped increase could be attributed to a dynamic feature of the framework material³⁴ or a preferential adsorption site.³⁵ The single crystal structure of pentaHOF-1 shows copper paddlewheels situated directly above each other with a Cu---Cu separation of 7.37 Å, which conforms well with a previously described "optimum" distance for the binding of CO_2 .³⁵ In the case of pentaHOF-1, the adsorption step occurs at much lower partial pressures than described in the literature, possibly indicating a stronger binding. The CO_2 isotherms of pentaMOF-2 and -3 described a type-I shape with a total uptake significantly smaller than pentaHOF-1. The differences in total CO_2 uptake between the three structures are in stark contrast to the available metal binding sites per gram of material. In pentaMOF-2 and -3 the available number of metal binding sites are the same, corresponding to 56.6 ml/g CO_2 . This value accounts nearly half of the adsorption,

considering the total uptake of 108.8 and 124.2 ml/g for pentaMOF-2 and -3, respectively. In pentaHOF-1, the metal adsorption sites account for only 16.0 ml/g CO_2 , which is small compared to the total uptake of 297.5 ml/g (~5% of the total uptake). In addition to the adsorption on the metal sites, the pore sizes of the materials are strongly influencing the adsorption properties of the materials. In pentaMOF-2 and -3 only small pores are present, while pentaHOF-1 has a much larger channel with a ~1.1 nm diameter in addition to small pores close to the metal centers. The small pores in the materials seem to reject N_2 , which explains why pentaMOF-2 and -3 show no uptake of nitrogen but a small uptake of CO_2 . On the other hand, it is surprising, that a hydrogen bonded structure of a metal containing molecular complex possesses larger porosity than the corresponding MOFs. Normally, the formation of metal-ligand bonds is the driving force that leads to porous MOF. However, in this case, the formation of pentaHOF-1 with a high porosity and low number of copper-ligand bonds is an unexpected outcome that can be linked to geometric frustration. We therefore systematically investigated structural constraints, to elucidate this peculiar behavior.

Effect of geometric frustration on the structures. Grason¹² offers a theoretical context for interpreting the effects of geometric frustration by defining anomalous structural properties such as "internally stressed equilibrium structures, self-limiting assembly, and topological defects in the equilibrium assembly structures".¹² All structures derived from the pL building block show these signs of frustration. In self-limiting equilibrium structures, the size of an assembly is limited, since the local interactions lead to stresses that sum up to limit the growth. In pentaHOF-1 this is observed in an extreme fashion as the molecule $Cu_2(pLH_4)_4$ consists of only the first sphere of coordination, as a single copper paddlewheel is surrounded by four pL molecules that are not connected to further metal SBU. This is surprising, since under the applied synthetic conditions, a full reaction could be expected, as it is possible to synthesize copper paddlewheel MOFs such as, for example, HKUST-1 at room temperature.²⁸

Internally stressed equilibrium structures arise, where the self-limiting growth is overcome and extended metal-ligand nets are formed. The high coordination number of the nodes and the rigid nature of the building blocks lead to few degrees of freedom for the system to form a stable structure. This leads to suboptimal coordination environments, as the angles and distances of the carboxylic acid groups cannot be rearranged to accommodate the energetic minimum for an unstrained copper paddlewheel. In pentaHOF-1, the copper paddlewheel (Figure 4) and the pL molecules are unstrained as a result of the formation of a discrete molecule. However, the structures of pentaMOF-2 and pentaMOF-3 show a copper paddlewheel that is more distorted than in any previously reported phenyl based copper paddlewheel structure in the Cambridge structural database³⁸ (CSD, 454 structures) (Figure 4, see method section). In pentaMOF-2 one paddlewheel remains largely unaffected by strain, while the other is

markedly distorted. The pentaMOF-3 structure shows one paddlewheel that is distorted more strongly than in pentaMOF-2 (Figure 4 blue circles), and additionally the second SBU is strained so strongly that the paddlewheel motif breaks down and a rod SBU is formed instead (Figure 2f, Figure 4 blue X). The copper SBU is experiencing strain in the equatorial plane and also in the axial direction (Figure 2f, Figure S13) as a consequence of the partially overlapping linkers (Figure 2e) within one layer of pentaMOF-3. The equatorial strain can be resolved by an in-plane change of the bite angle (Figure S14), while the axial strain is released by altering the binding motif from a paddlewheel to a rod SBU. This effect can be quantified by calculating the out-of-plane distortion of the [pLH]⁴ carboxyphenyl groups in relation to the central pyrrole core. The groups connected to the rod SBU show a significantly reduced out-of-plane bending compared to those connected to the copper paddlewheels (Figure S15, Table S3). The internal stress of the structures can also be observed in the hydrogen bonding in pentaHOF-1 and pentaMOF-3, where the disorder of the free carboxylic acids suggests competition between two hydrogen bonding states. In pentaHOF-1, one state with three hydrogen bonds between four carboxylic acids (Figure S4b, d) competes with a state where two pairs of carboxylic acids can form one hydrogen bond each (Figure S4c). In pentaMOF-3, the two binding modes are characterized by a carboxylic acid dimer with two hydrogen bonds and a carboxylic acid dimer with only one hydrogen bond (Figure S8). The rigid backbone prohibits the complete relaxation of the structure to maximize the number of hydrogen bonds, leading to strained hydrogen bonding interactions.

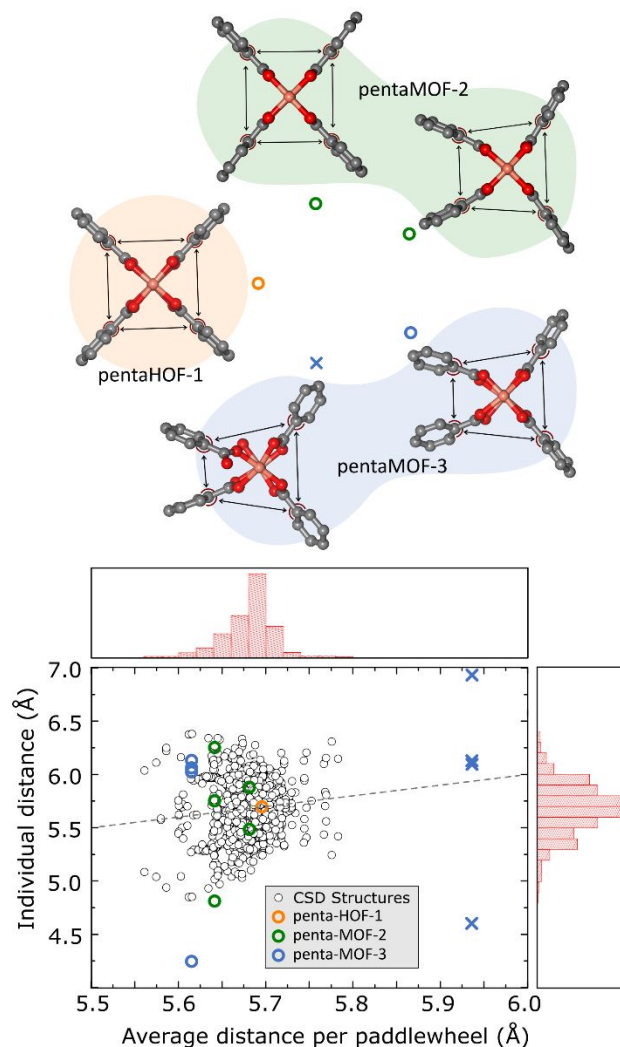


Figure 4. Distortion of the copper paddlewheel structure of pentaHOF-1, pentaMOF-2 and pentaMOF-3, in comparison to structures reported in the Cambridge Structural Database. As assessed by the carbon distances as indicated in the top. The dashes line indicates values where $x=y$.

Dangling carboxylic acid groups remain in the structures of pentaMOF-2 and -3, even as the number of ligand-to-copper bonds are increased compared to pentaHOF-1. These topological defects in the equilibrium structure lead to coordination nets based on a 4-c node for the nominally 5-c pLH₅ linker (Figure 2e). This can be understood as a result of the difficulty translating the C₅ symmetry of the linker to a periodic pattern. Additionally, the high but unequal number of points of extension leads to an overload in points of extension already in the first sphere of reticulation, which is then resolved by dangling carboxylic acids.

Applying this analysis to other reported MOFs, reveals geometric frustration leading to anomalous structures such as in the formation of a hydrogen bonded material consisting of metal organic polyhedra instead of a MOF³⁹ and the formation distorted or

untypical metal SBU due to incompatibilities between the linker and the SBU (see also supplemental discussion).⁴⁰

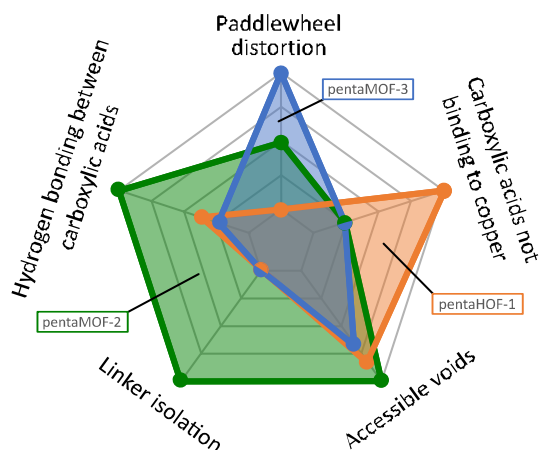


Figure 5. Qualitative assessment of the competing forces that lead to frustration (details can be found in Figure S16). Values further from the center indicate a stronger penalty.

The hallmark of geometric frustration is the absence of a simple ground state, which leads to structural solutions that show compromises of competing driving forces; metal-to-ligand bonding, metal coordination environment, hydrogen bonding, hydrophobic interactions, porosity and geometric constraints of the linker. The described system follows divergent pathways to trade-off several dimensions of structural degrees of freedom to release some of the frustration; five of the most prominent are shown in Figure 5. Each structure occupies a different area in this qualitative frustration diagram, illustrating the structural trade-offs. The driving force in MOF formation is the formation of the metal-ligand bond, yet protonated carboxylic acids remain in the resulting structures to different extent. In pentaHOF-1, only one of five carboxylate groups bind to copper and in pentaMOF-2 and -3, four out of five carboxylic acids bind to copper. At the same time, the distortion of the copper paddlewheels, which also carries a large penalty, follows the opposite trend: pentaHOF-1 has a copper paddlewheel without distortion, while in pentaMOF-2 and -3 some or all of the paddlewheel motifs are distorted. Comparing the pentaMOF-2 to -3, the number of free carboxylic acids are the same, but a trade-off can be observed between the paddlewheel distortion and the remaining three factors: hydrogen bonding, linker isolation, and accessible voids. The paddlewheel distortion is the largest in pentaMOF-3, but the free carboxylic acids are able to participate in hydrogen bonding unlike in pentaMOF-2, where the carboxylic acids are completely isolated. The linkers within the MOF backbone are also much more isolated in pentaMOF-2 than in pentaMOF-3, which also leads to an increased solvent accessible surface in pentaMOF-2. Consequently, the penalty from the isolation of the backbone in pentaMOF-2, allows it to reduce the distortion of the paddlewheels, and vice versa in pentaMOF-3. These results indicate that the

comparatively weak interactions between linkers play a significant role in determining the structure of both MOFs. The diagram also reveals that some structural features can completely relax in some structures, such as the completely undistorted paddlewheel in pentaHOF-1. Other features such as the carboxylate binding to copper is at a maximum 4/5 per pL linker, thus not binding to metals.

CONCLUSION

We have reported three porous materials in a frustrated linker - metal node system. The geometry of the linker and the combination of a nominally 5-c with a 4-c node induced geometric frustration that manifested in the distorted linkers and nodes, sub-stoichiometry, and porosity. The analysis of the linker distortion was used as a qualitative basis to evaluate the frustration in the obtained structures. The structures reported here point towards using geometrically frustrated assembly as a design principle in reticular materials to form metal containing HOFs, unusual metal SBUs, dangling functional groups and polymorphic structures.

ASSOCIATED CONTENT

Supporting Information The Supporting Information is available free of charge on the ACS Publications website at DOI:.

Materials and methods; Supplementary Figures S1–S32, Supplementary Tables S1–S3 containing SRXD data, PXRD, TGA and additional information about the nets. (PDF)

Single Crystal X-ray Data for pentaHOF-1 (CCDC: 1991981)

Single Crystal X-ray Data for pentaMOF-2 (CCDC: 1991980)

Single Crystal X-ray Data for pentaMOF-3 (CCDC: 1991982)

AUTHOR INFORMATION

Corresponding Author

To whom correspondence should be addressed:
shuhei.furukawa@icems.kyoto-u.ac.jp
haase.frederik.35c@st.kyoto-u.ac.jp

Notes

The authors declare no competing financial interests.

ACKNOWLEDGMENT

F.H. is grateful to the Japan Society for the Promotion of Science (JSPS) for Post-Doctoral Fellowships. The authors acknowledge iCeMS Analysis Center for access to analytical facilities.

REFERENCES

- (1) Guillerm, V.; Maspoch, D. Geometry Mismatch and Reticular Chemistry: Strategies To Assemble Metal–Organic Frameworks with Non-Default Topologies. *J. Am. Chem. Soc.* **2019**, *141* (42), 16517–16538.
- (2) Furukawa, H.; Cordova, K. E.; O’Keeffe, M.; Yaghi, O. M. The Chemistry and Applications of Metal–Organic Frameworks. *Science* **2013**, *341* (6149).
- (3) Chen, Z.; Thiam, Z.; Shkurenko, A.; Weselinski, L. J.; Adil, K.; Jiang, H.; Alezi, D.; Assen, A. H.; O’Keeffe, M.; Eddaoudi, M. Enriching the Reticular Chemistry Repertoire with

Minimal Edge-Transitive Related Nets: Access to Highly Coordinated Metal–Organic Frameworks Based on Double Six-Membered Rings as Net-Coded Building Units. *J. Am. Chem. Soc.* **2019**, *141* (51), 20480–20489.

(4) Tu, B.; Diestel, L.; Shi, Z.-L.; Bandara, W. R. L. N.; Chen, Y.; Lin, W.; Zhang, Y.-B.; Telfer, S. G.; Li, Q. Harnessing Bottom-Up Self-Assembly To Position Five Distinct Components in an Ordered Porous Framework. *Angew. Chem.* **2019**, *131* (16), 5402–5407.

(5) Tu, B.; Diestel, L.; Shi, Z.-L.; Bandara, W. R. L. N.; Chen, Y.; Lin, W.; Zhang, Y.-B.; Telfer, S. G.; Li, Q. Harnessing Bottom-Up Self-Assembly To Position Five Distinct Components in an Ordered Porous Framework. *Angew. Chem. Int. Ed.* **2019**, *58* (16), 5348–5353.

(6) Zhou, T.-Y.; Auer, B.; Lee, S. J.; Telfer, S. G. Catalysts Confined in Programmed Framework Pores Enable New Transformations and Tune Reaction Efficiency and Selectivity. *J. Am. Chem. Soc.* **2019**, *141* (4), 1577–1582.

(7) Tu, B.; Pang, Q.; Wu, D.; Song, Y.; Weng, L.; Li, Q. Ordered Vacancies and Their Chemistry in Metal–Organic Frameworks. *J. Am. Chem. Soc.* **2014**, *136* (41), 14465–14471.

(8) Park, H.; Kim, S.; Jung, B.; Park, M. H.; Kim, Y.; Kim, M. Defect Engineering into Metal–Organic Frameworks for the Rapid and Sequential Installation of Functionalities. *Inorg. Chem.* **2018**, *57* (3), 1040–1047.

(9) Ling, S.; Slater, B. Dynamic Acidity in Defective UiO-66. *Chem. Sci.* **2016**, *7* (7), 4706–4712.

(10) Xue, Z.; Liu, K.; Liu, Q.; Li, Y.; Li, M.; Su, C.-Y.; Ogiwara, N.; Kobayashi, H.; Kitagawa, H.; Liu, M.; Li, G. Missing-Linker Metal–Organic Frameworks for Oxygen Evolution Reaction. *Nat. Commun.* **2019**, *10* (1), 5048.

(11) Firth, F. C. N.; Cliffe, M. J.; Vulpe, D.; Aragonés-Anglada, M.; Moghadam, P. Z.; Fairen-Jimenez, D.; Slater, B.; Grey, C. P. Engineering New Defective Phases of UiO Family Metal–Organic Frameworks with Water. *J. Mater. Chem. A* **2019**, *7* (13), 7459–7469.

(12) Grason, G. M. Perspective: Geometrically Frustrated Assemblies. *J. Chem. Phys.* **2016**, *145* (11), 110901.

(13) Bramwell, S. T.; Gingras, M. J. P. Spin Ice State in Frustrated Magnetic Pyrochlore Materials. *Science* **2001**, *294* (5546), 1495–1501.

(14) Nisoli, C.; Moessner, R.; Schiffer, P. Colloquium: Artificial Spin Ice: Designing and Imaging Magnetic Frustration. *Rev. Mod. Phys.* **2013**, *85* (4), 1473–1490.

(15) Gibbs, W. W. A New Form of Pure Carbon Dazzles and Attracts. *Science* **2019**, *366* (6467), 782–783.

(16) Liu, L.; Li, Z.; Li, Y.; Mao, C. Rational Design and Self-Assembly of Two-Dimensional, Dodecahedral DNA Quasicrystals. *J. Am. Chem. Soc.* **2019**, *141* (10), 4248–4251.

(17) Lee, S.; Chen, C.-H.; Flood, A. H. A Pentagonal Cyanostar Macrocyclic with Cyanostilbene CH Donors Binds Anions and Forms Dialkylphosphate [3]Rotaxanes. *Nat. Chem.* **2013**, *5* (8), 704–710.

(18) Jon, S. Y.; Selvapalam, N.; Oh, D. H.; Kang, J.-K.; Kim, S.-Y.; Jeon, Y. J.; Lee, J. W.; Kim, K. Facile Synthesis of Cucurbit[n]uril Derivatives via Direct Functionalization: Expanding Utilization of Cucurbit[n]uril. *J. Am. Chem. Soc.* **2003**, *125* (34), 10186–10187.

(19) Less, R. J.; Wilson, T. C.; Guan, B.; McPartlin, M.; Steiner, A.; Wood, P. T.; Wright, D. S. Solvent Direction of Molecular Architectures in Group 1 Metal Pentacyanocyclopentadienides. *Eur. J. Inorg. Chem.* **2013**, *2013* (7), 1161–1169.

(20) Chen, Y.-S.; Solel, E.; Huang, Y.-F.; Wang, C.-L.; Tu, T.-H.; Keinan, E.; Chan, Y.-T. Chemical Mimicry of Viral Capsid Self-Assembly via Corannulene-Based Pentatopic Tectons. *Nat. Commun.* **2019**, *10* (1), 3443.

(21) Tong, L. H.; Guénee, L.; Williams, A. F. Pentasubstituted Ferrocene and Dirhodium(II) Tetracarboxylate as Building Blocks for Discrete Fullerene-Like and Extended

Supramolecular Structures. *Inorg. Chem.* **2011**, *50* (6), 2450–2457.

(22) Bacsá, J.; Less, R. J.; Skelton, H. E.; Soracevic, Z.; Steiner, A.; Wilson, T. C.; Wood, P. T.; Wright, D. S. Assembly of the First Fullerene-Type Metal–Organic Frameworks Using a Planar Five-Fold Coordination Node. *Angew. Chem. Int. Ed.* **2011**, *50* (36), 8279–8282.

(23) Bacsá, J.; Less, R. J.; Skelton, H. E.; Soracevic, Z.; Steiner, A.; Wilson, T. C.; Wood, P. T.; Wright, D. S. Assembly of the First Fullerene-Type Metal–Organic Frameworks Using a Planar Five-Fold Coordination Node. *Angew. Chem.* **2011**, *123* (36), 8429–8432.

(24) Nam, S.; Ware, D. C.; Brothers, P. J. Macrocyclic Pentamers Functionalised around Their Periphery as Potential Building Blocks. *RSC Adv.* **2019**, *9* (15), 8389–8393.

(25) Smetana, V.; Kelley, S. P.; Mudring, A.-V.; Rogers, R. D. A Fivefold UO₂²⁺ Node Is a Path to Dodecahedral Quasicrystal Approximants in Coordination Polymers. *Sci. Adv.* **2020**, *6* (5), eaay7685.

(26) Oms, O.; Jarrosson, T.; Tong, L. H.; Vaccaro, A.; Bernardinelli, G.; Williams, A. F. Synthesis of Planar Five-Connected Nodal Ligands. *Chem. – Eur. J.* **2009**, *15* (20), 5012–5022.

(27) Eddaoudi, M.; Kim, J.; O’Keeffe, M.; Yaghi, O. M. Cu₂[o-Br-C₆H₃(CO₂)₂]₂(H₂O)₂·(DMF)₈(H₂O)₂: A Framework Deliberately Designed To Have the NbO Structure Type. *J. Am. Chem. Soc.* **2002**, *124* (3), 376–377.

(28) Chen, Y.; Mu, X.; Lester, E.; Wu, T. High Efficiency Synthesis of HKUST-1 under Mild Conditions with High BET Surface Area and CO₂ Uptake Capacity. *Prog. Nat. Sci. Mater. Int.* **2018**, *28* (5), 584–589.

(29) Stylianou, K. C.; Rabone, J.; Chong, S. Y.; Heck, R.; Armstrong, J.; Wiper, P. V.; Jelfs, K. E.; Zlatogorsky, S.; Bacsá, J.; McLennan, A. G.; Ireland, C. P.; Khimyak, Y. Z.; Thomas, K. M.; Bradshaw, D.; Rosseinsky, M. J. Dimensionality Transformation through Paddlewheel Reconfiguration in a Flexible and Porous Zn-Based Metal–Organic Framework. *J. Am. Chem. Soc.* **2012**, *134* (50), 20466–20478.

(30) Gómez-Gualdrón, D. A.; Colón, Y. J.; Zhang, X.; Wang, T. C.; Chen, Y.-S.; Hupp, J. T.; Yildirim, T.; Farha, O. K.; Zhang, J.; Snurr, R. Q. Evaluating Topologically Diverse Metal–Organic Frameworks for Cryo-Adsorbed Hydrogen Storage. *Energy Environ. Sci.* **2016**, *9* (10), 3279–3289.

(31) O’Keeffe, M.; Peskov, M. A.; Ramsden, S. J.; Yaghi, O. M. The Reticular Chemistry Structure Resource (RCSR) Database of, and Symbols for, Crystal Nets. *Acc. Chem. Res.* **2008**, *41* (12), 1782–1789.

(32) Lin, R.-B.; He, Y.; Li, P.; Wang, H.; Zhou, W.; Chen, B. Multifunctional Porous Hydrogen-Bonded Organic Framework Materials. *Chem. Soc. Rev.* **2019**, *48* (5), 1362–1389.

(33) Ramsden, S. J.; Robins, V.; Hyde, S. T.; Hungerford, S. EPINET: Euclidean Patterns in Non-Euclidean Tilings. 2005–2009. The Australian National University. <http://epinet.anu.edu.au/>.

(34) Kondo, A.; Noguchi, H.; Carlucci, L.; Proserpio, D. M.; Ciani, G.; Kajiro, H.; Ohba, T.; Kanoh, H.; Kaneko, K. Double-Step Gas Sorption of a Two-Dimensional Metal–Organic Framework. *J. Am. Chem. Soc.* **2007**, *129* (41), 12362–12363.

(35) Li, J.-R.; Yu, J.; Lu, W.; Sun, L.-B.; Sculley, J.; Balbuena, P. B.; Zhou, H.-C. Porous Materials with Pre-Designed Single-Molecule Traps for CO₂ Selective Adsorption. *Nat. Commun.* **2013**, *4*, 1538.

(36) Sumida, K.; Rogow, D. L.; Mason, J. A.; McDonald, T. M.; Bloch, E. D.; Herm, Z. R.; Bae, T.-H.; Long, J. R. Carbon Dioxide Capture in Metal–Organic Frameworks. *Chem. Rev.* **2012**, *112* (2), 724–781.

(37) Delgado-Friedrichs, O.; O’Keeffe, M.; Yaghi, O. M.

1 Three-Periodic Nets and Tilings: Edge-Transitive Binodal
2 Structures. *Acta Crystallogr. A* **2006**, *62* (5), 350–355.

3 (38) Groom, C. R.; Bruno, I. J.; Lightfoot, M. P.; Ward, S.
4 C. The Cambridge Structural Database. *Acta Crystallogr. Sect.*
5 *B Struct. Sci. Cryst. Eng. Mater.* **2016**, *72* (2), 171–179.

6 (39) Gong, W.; Chu, D.; Jiang, H.; Chen, X.; Cui, Y.; Liu,
7 Y. Permanent Porous Hydrogen-Bonded Frameworks with Two
8 Types of Brønsted Acid Sites for Heterogeneous Asymmetric
9 Catalysis. *Nat. Commun.* **2019**, *10* (1), 600.

10 (40) Wong-Foy, A. G.; Lebel, O.; Matzger, A. J. Porous
11 Crystal Derived from a Tricarboxylate Linker with Two Distinct
12 Binding Motifs. *J. Am. Chem. Soc.* **2007**, *129* (51), 15740–
13 15741.

14 (41) Dolomanov, O. V.; Bourhis, L. J.; Gildea, R. J.;
15 Howard, J. a. K.; Puschmann, H. OLEX2: A Complete Structure
16 Solution, Refinement and Analysis Program. *J. Appl.*
17 *Crystallogr.* **2009**, *42* (2), 339–341.

18 (42) Sheldrick, G. M. A Short History of SHELX. *Acta*
19 *Crystallogr. A* **2008**, *64* (1), 112–122.

20 (43) Sheldrick, G. M. Crystal Structure Refinement with
21 SHELXL. *Acta Crystallogr. Sect. C Struct. Chem.* **2015**, *71* (1),
22 3–8.

23 (44) Spek, A. L. PLATON SQUEEZE: A Tool for the
24 Calculation of the Disordered Solvent Contribution to the
25 Calculated Structure Factors. *Acta Crystallogr. Sect. C Struct.*
26 *Chem.* **2015**, *71* (1), 9–18.

27 (45) Spek, A. L. Structure Validation in Chemical
28 Crystallography. *Acta Crystallogr. D Biol. Crystallogr.* **2009**, *65*
29 (2), 148–155.

30 (46) Blatov, V. A.; Shevchenko, A. P.; Proserpio, D. M.
31 Applied Topological Analysis of Crystal Structures with the
32 Program Package ToposPro. *Cryst. Growth Des.* **2014**, *14* (7),
33 3576–3586.

